doi: 10.12029/gc2020Z105

论文引用格式：任邦方, 段连峰, 李敏, 牛文超, 任云伟. 2020. 内蒙古北山哈珠地区晚古生代花岗岩类年代学与地球化学测试数据集 [J].中国地质，47(S1):40–49.

数据集引用格式：任邦方; 段连峰; 李敏; 牛文超; 任云伟. 内蒙古北山哈珠地区晚古生代花岗岩类年代学与地球化学测试数据集 (V1).中国地质调查局天津地质调查中心 [创建机构]，2014. 全国地质资料馆 [传播机构]. 2020-06-30.10.35080/data.A.2020.P5; http://dcc.cgs.gov.cn/cn//geologicalData/details/doi/10.35080/data.A.2020.P5

收稿日期：2020-04-08
改回日期：2020-04-27

基金项目：中国地质调查局地质调查项目（DD20160039、DD20190382）联合资助。

内蒙古北山哈珠地区晚古生代花岗岩类年代学与地球化学测试数据集

任邦方　段连峰　李敏　牛文超*　任云伟

(中国地质调查局天津地质调查中心，天津 300170)

摘要：本数据集依托中国地质调查局“内蒙古 1∶50 000 哈珠幅、哈珠东山幅、哈珠南山幅和砾石滩幅区域地质矿产调查”项目，在详细开展野外地质调查的基础上，进行岩石分析测试整理而成。本文汇集了内蒙古北山哈珠地区晚古生代花岗岩类样品的测试数据，岩石类型包括英云闪长岩、花岗闪长岩、二长花岗岩和碱性长石花岗岩。锆石年代学数据显示该类岩石的形成时代为石炭纪–二叠纪，岩石全岩常量和微量元素数据表明石炭纪花岗岩类为准铝质–弱过铝质、中钾钙碱性系列岩石；稀土元素配分曲线呈现右倾分布特征；微量元素富集大离子亲石元素 Rb、Ba、K 等，亏损 Nb、Ta、Ti 等高场强元素，反映了岩浆形成于与俯冲带有关的陆缘弧环境。而二叠纪花岗岩类则表现为高硅、富碱、准铝、贫镁的特征，为中钾–高钾钙碱性系列岩石；该类岩石同样表现为富集大离子亲石元素，亏损高场强元素，但碱性长石花岗岩内发育文象结构，且花岗闪长岩内发育大规模水晶晶洞，指示二叠纪岩体就位于伸展环境。两者相结合可以为研究北山地区红石山–百合山洋的俯冲极性及构造演化提供依据与基础数据支持。本数据集为 Excel 表格型数据，包括 2 个 .xls 类型文件（Geochemistry data_HZ.xls，Zircon U–Pb dating data_HZ.xls），分别记录了 27 件样品的地球化学数据与 11 件样品的锆石 U–Pb 测年数据。本数据集测试样品均在中国地质调查局天津地质调查中心实验室完成，数据质量可靠。

关键词：北山；哈珠；花岗岩；石炭纪–二叠纪；全岩地球化学数据；锆石 U–Pb 数据

数据服务系统网址：http://dcc.cgs.gov.cn

1　引言

北山造山带位于中亚造山带中段南缘，处于塔里木–华北板块、哈萨克斯坦板块和西伯利亚板块的交会部位（左国朝等，2003；图 1）。由于其经历了多期次、多阶段的

第一作者简介：任邦方，男，1981 年生，高级工程师，主要从事基础地质和地球化学研究；E–mail：bangfangren@foxmail.com。

通讯作者简介：牛文超，男，1986 年生，工程师，主要从事区域地质调查和造山带研究工作；E–mail：billynu2003@163.com。

板块裂解–俯冲–碰撞–拼合等复杂的地质演化过程，因此该地区的构造单元划分、古亚洲洋闭合时限等问题一直备受国内外学者关注（聂凤军等，2002；龚全胜等，2003；徐学义等，2008；Xiao WJ et al.，2010；杨合群等，2010；卢进才等，2013）。前人对北山地区构造单元划分主要有 4 种观点：（1）以明水–石板井–小黄山缝合带为界，北侧为哈萨克斯坦板块，南侧为塔里木板块（左国朝等，1990）；（2）以红柳河–牛圈子–洗肠井蛇绿岩带为界，南侧为塔里木板块，北侧为哈萨克斯坦板块（徐学义等，2008；杨合群等，2008；胡新茁等，2015；孙立新等，2017）；（3）以红石山–黑鹰山和柳园–大奇山为界，自北向南依次划分为西伯利亚板块、哈萨克斯坦板块和塔里木板块（聂凤军等，2003）；（4）以红石山–百合山–蓬勃山蛇绿岩带为界，北侧为哈萨克斯坦板块，南侧为塔里木板块（何世平等，2002；龚全胜等，2003）。近年来随着地质填图与调查研究的深入，多数学者对北山地区早古生代蛇绿岩带构造属性的认识逐渐趋于一致，认为红柳河–牛圈子–洗肠井蛇绿岩带为塔里木板块与哈萨克斯坦板块的早古生代缝合带，具有区域构造分区意义（徐学义等，2008；杨合群等，2008；胡新茁等，2015；廖云峰等，2016；孙立新等，2017）。但对于晚古生代红石山–百合山蛇绿岩带的构造属性及其是否具有缝合带的性质等一直存在较大的争议（左国朝等，1990；龚全胜等，2002；何世平等，2005；黄增保和金霞，2006；杨合群等，2010；王国强等，2014）。而对出露在红石山–百合山蛇绿岩带两侧的晚古生代岩浆岩开展研究，可以为进一步认识红石山–百合山蛇绿岩带的俯冲极性及地质演化提供重要的依据。因此，笔者依托 1∶50 000 哈珠幅、哈珠东山幅、哈珠南山幅和砾石滩幅区域地质调查项目，利用高精度分析测试手段，对出露在红石山–百合山蛇绿岩带南侧哈珠地区的晚古生代花岗岩类开展岩石学、地球化学及锆石 U–Pb 年代学研究，进而形成了本数据集。

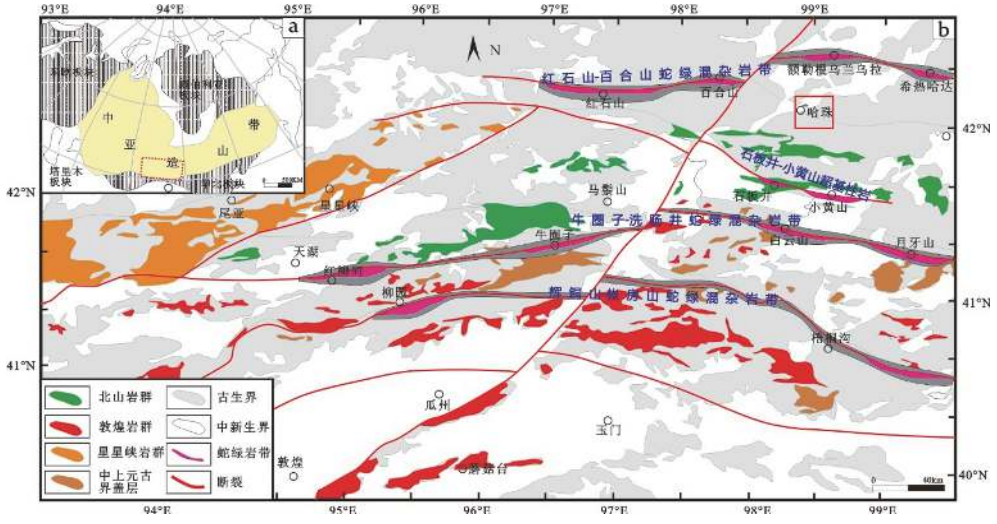

图 1　北山地区构造单元划分及研究区位置（图 a 据 Xiao et al., 2010；图 b 据牛文超等,2019）

哈珠一带晚古生代花岗岩类主要形成于晚石炭世和早二叠世。晚石炭世花岗岩类的岩石类型主要为英云闪长岩、花岗闪长岩和二长花岗岩，而早二叠世花岗岩类的岩石类型主要为碱性长石花岗岩、二长花岗岩和花岗闪长岩（图 2）。晚石炭世英云闪长岩出露面积较小，呈岩株产出，侵入下石炭统绿条山组，被晚石炭世花岗闪长岩和二叠纪花岗岩侵入。晚石炭世花岗闪长岩呈岩基产出，NW–SE 向面状展布，侵入绿条山组和白山组中，其内发育大量暗色基性微粒包体，与寄主岩的界线多呈截然，少数呈过渡关

系。晚石炭世二长花岗岩主要侵入花岗闪长岩以及绿条山组、白山组中，并被早二叠世二长花岗岩侵入。早二叠世二长花岗岩和中二叠世花岗闪长岩出露规模较大，呈岩基状产出，空间上两者共同构成一个大型椭球体，其中二长花岗岩位于椭球体两侧，花岗闪长岩位于椭球体中心，花岗闪长岩侵入二长花岗岩中（图 3）。受区域构造影响，该椭球体长轴方向呈 NWW 向。岩体风化强烈，球形风化及洞状风蚀岩貌特征明显，并可见

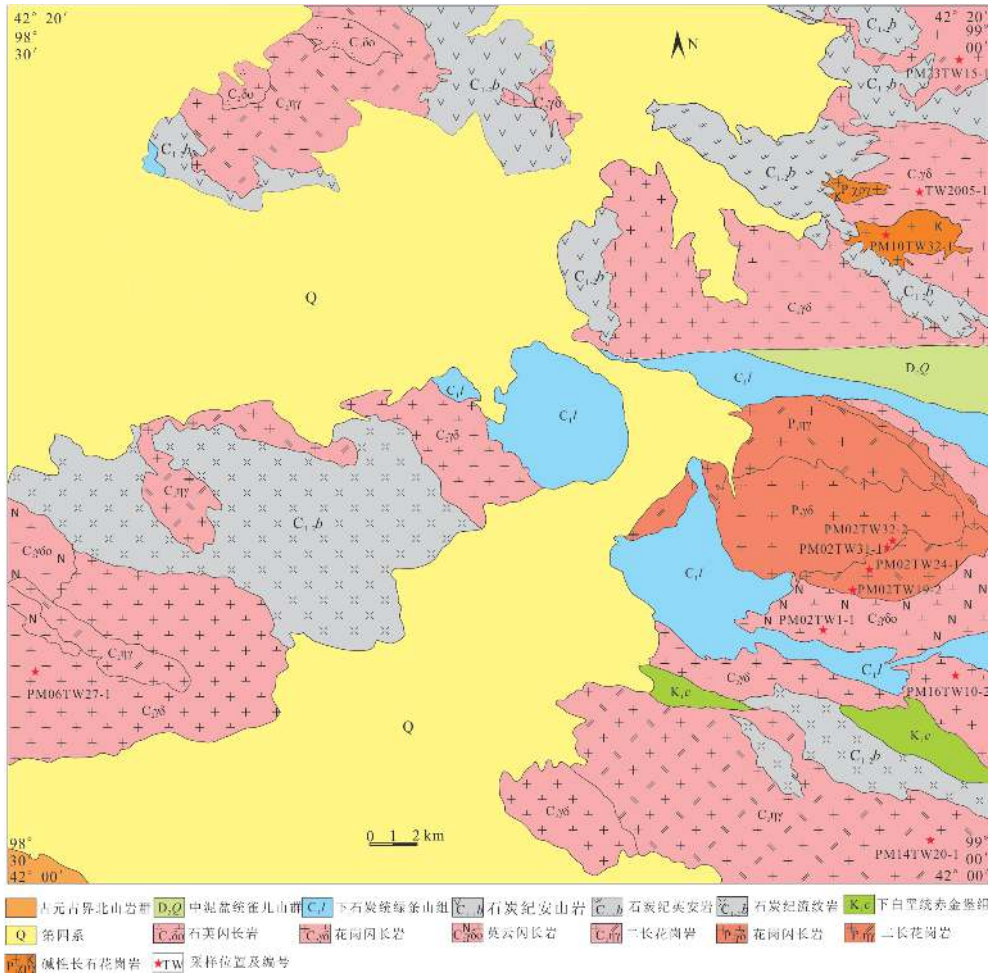

图 2　内蒙古北山哈珠地区地质简图及同位素测年样品采样位置
（据内蒙古 1∶50 000 哈珠等 4 幅区域地质图修编）

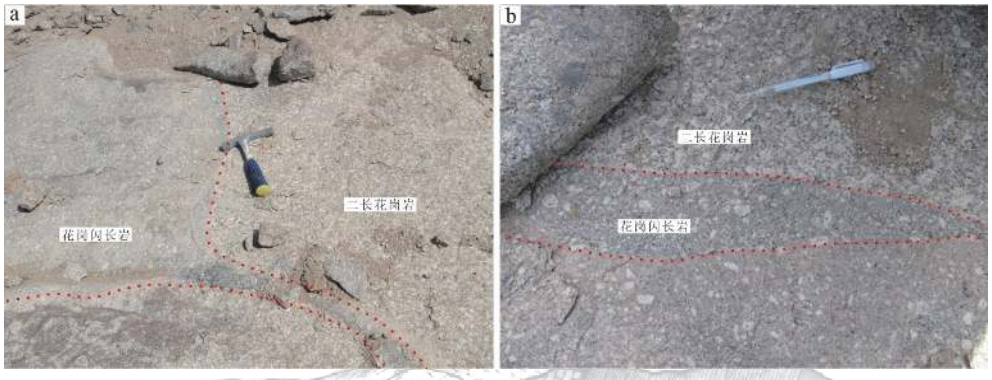

图 3　内蒙古北山哈珠地区早二叠世花岗闪长岩和二长花岗岩接触关系
（图 a 花岗闪长岩侵入二长花岗岩中；图 b 侵入二长花岗岩中的花岗闪长岩岩枝）

大量水晶晶洞。岩体内暗色闪长质包体发育，个别闪长质包体内可见白色长石粗晶。研究区内早二叠世碱性长石花岗岩出露面积较小，呈小岩株状产出，侵入石炭纪花岗岩和白山组火山岩中。

哈珠地区晚古生代花岗岩类锆石年代学与全岩地球化学测试数据集（任邦方等，2020）元数据简表见表 1。

表 1　数据集元数据简表

条目	描述
数据集名称	内蒙古北山哈珠地区晚古生代花岗岩类年代学与地球化学测试数据集
数据集作者	任邦方，中国地质调查局天津地质调查中心 段连峰，中国地质调查局天津地质调查中心 李　敏，中国地质调查局天津地质调查中心 牛文超，中国地质调查局天津地质调查中心 任云伟，中国地质调查局天津地质调查中心
数据时间范围	2014–2016年
地理区域	42°00′00″ ~ 42°20′00″，98°30′00″ ~ 99°00′00″
数据格式	*.xls
数据量	140 KB
数据服务系统网址	http://dcc.cgs.gov.cn
基金项目	中国地质调查局地质调查项目（DD20160039，DD20190382）
语种	中文
数据库（集）组成	数据集由2部分组成：（1）Geochemistry data_HZ.xls，为全岩地球化学数据，包括27件样品以及样品编号与岩石类型；（2）Zircon U–Pb dating data_HZ.xls，为锆石U-Pb测年数据，包括11件样品，每个样品为一个单独的工作表（sheet），每个工作表包含样品编号、采样点、岩石类型、分析点号、同位素比值、年龄及误差等数据

2　数据采集和处理方法

2.1　数据采集

本次研究所采集的岩石样品为内蒙古北山哈珠地区晚石炭世–早二叠世花岗岩类，共 27 件，其中 9 件样品进行了锆石 U–Pb 测年和岩石地球化学分析，2 件样品只进行了锆石 U–Pb 测年，18 件样品只进行了岩石地球化学分析。岩石类型包括英云闪长岩、花岗闪长岩、二长花岗岩和碱性长石花岗岩。岩石的采样地点与具体的矿物组合见表 2，矿物简称采用 Whitney DL et al.(2010) 的方案。

2.2　样品采集、制作和测试方法

本次研究用于测试的花岗岩类样品均是在野外路线调查和剖面实测的基础上系统采集的。测年样品的粉碎加工、锆石分选在河北省区域地质矿产调查研究所实验室完成，样品破碎到 40 ~ 60 目，经过磁选和重液分离后，借助双目镜人工挑选干净和自形程度较高，包裹体和裂隙少的锆石颗粒制成环氧树脂样品靶。制靶和锆石阴极发光照相在北京锆年领航科技有限公司完成。在对锆石外观特征分析研究的基础上，选取具有明显岩浆振荡环带结构且无裂隙和包裹体的锆石进行测试。LA–ICP–MS 锆石微区 U–Pb 同位素测定在中国地质调查局天津地质调查中心同位素实验室进行，所用激光器为 NEWWAVE 193 nm FX，质谱仪为 Thermo Fisher 公司的 NEPTUNE（耿建珍等，2011）。分析采用

表 2 哈珠地区花岗岩类样品采样地点及矿物组合

样品号	采集地点	岩石类型	矿物组合
PM02YQ19-2	内蒙古哈珠地区砾石滩	二长花岗岩	kfs(40%±), pl(35%), qtz(20%±), bt(3%±), hbl(2%±)
PM02YQ24-1	内蒙古哈珠地区砾石滩	二长花岗岩	pl(40%±), kfs(30%±), qtz(20%±), bt(5%±), hbl(2%±)
PM02YQ25-2	内蒙古哈珠地区砾石滩	花岗闪长岩	pl(45%±), kfs(25%±), qtz(20%±), hbl(5%±), bt(3%±)
PM02YQ31-1	内蒙古哈珠地区砾石滩	花岗闪长岩	pl(45%±), qtz(35%±), kfs(15%±), hbl(5%±)
PM02YQ32-1	内蒙古哈珠地区砾石滩	花岗闪长岩	pl(50%±), qtz(25%±), kfs(15%±), hbl(5%±), bt(2%±)
PM02YQ32-2	内蒙古哈珠地区砾石滩	花岗闪长岩	pl(50%±), kfs(20%±), qtz(20%±), hbl(5%±), bt(3%±)
PM02YQ33-2	内蒙古哈珠地区砾石滩	花岗闪长岩	pl(45%±), qtz(25%±), kfs(20%±), bt(5%±), hbl(3%±)
PM02YQ38-1	内蒙古哈珠地区砾石滩	花岗闪长岩	pl(50%±), kfs(25%±), qtz(20%±), hbl(5%±), bt(2%±)
PM02YQ39-1	内蒙古哈珠地区砾石滩	二长花岗岩	pl(40%±), kfs(30%±), qtz(20%±), hbl(5%±), bt(3%±)
PM02YQ40-2	内蒙古哈珠地区砾石滩	二长花岗岩	pl(35%±), kfs(35%±), qtz(25%±), hbl(3%±), bt(2%±)
PM02YQ42-1	内蒙古哈珠地区砾石滩	英云闪长岩	pl(55%±), qtz(30%±), bt(8%±), kfs(5%±), hbl(2%±),
PM02YQ44-1	内蒙古哈珠地区砾石滩	英云闪长岩	pl(60%±), qtz(25%±), kfs(5%±), hbl(5%±), bt(5%±)
PM02YQ45-1	内蒙古哈珠地区砾石滩	英云闪长岩	pl(55%±), qtz(30%±), kfs(5%±), hbl(5%±), bt(5%±)
YQ7907-1	内蒙古哈珠地区砾石滩	花岗闪长岩	pl(50%±), qtz(25%±), kfs(20%±), hbl(5%±), bt(2%±)
YQ7965-2	内蒙古哈珠地区砾石滩	花岗闪长岩	pl(45%±), qtz(25%±), kfs(20%±), hbl(5%±), bt(3%±)
PM06YQ20-1	内蒙古哈珠南山	花岗闪长岩	pl(60%±), qtz(20%±), kfs(15%±), bt(5%±)
PM06YQ27-1	内蒙古哈珠南山	花岗闪长岩	pl(55%±), qtz(25%±), kfs(15%±), bt(5%±)
PM10YQ32-1	内蒙古哈珠地区砾石滩	碱性长石花岗岩	af(60%±), qtz(35%±), bt(5%±)
PM16YQ1-1	内蒙古哈珠南山	花岗闪长岩	pl(40%±), qtz(30%±), hbl(15%±), kfs(10%±), bt(5%±)
PM16YQ2-1	内蒙古哈珠南山	花岗闪长岩	pl(50%±), qtz(20%±), kfs(10%±), hbl(10%±), bt(8%±)
PM16YQ3-1	内蒙古哈珠南山	花岗闪长岩	pl(50%±), qtz(20%±), kfs(15%±), hbl(10%±), bt(5%±)
PM16YQ10-1	内蒙古哈珠南山	花岗闪长岩	pl(55%±), qtz(20%±), kfs(10%±), hbl(10%±), bt(5%±)
PM16YQ10-2	内蒙古哈珠南山	花岗闪长岩	pl(50%±), qtz(20%±), kfs(10%±), bt(10%±), hbl(8%±)
PM23YQ15-1	内蒙古哈珠东山	花岗闪长岩	pl(50%±), qtz(20%±), kfs(15%±), hbl(10%±), bt(5%±)
YQ11	内蒙古哈珠地区砾石滩	二长花岗岩	pl(35%±), kfs(35%±), qtz(25%±), hbl(3%±), bt(2%±)
YQ12	内蒙古哈珠地区砾石滩	二长花岗岩	pl(40%±), kfs(30%±), qtz(20%±), hbl(5%±), bt(3%±)
YQ2005-1	内蒙古哈珠东山	花岗闪长岩	pl(40%±), qtz(30%±), hbl(15%±), kfs(10%±), bt(5%±)

注：af–碱性长石；bt–黑云母；hbl–角闪石；kfs–钾长石；pl–斜长石；qtz–石英

的激光束斑直径 35 μm，频率 8 ~ 10 Hz，激光器能量密度 13 ~ 14 J / cm^2，以氦气作为剥蚀物质的载气，分析流程见 Yuan HL et al.(2004)。实验中利用 NIST612 玻璃标样作为外标进行仪器最优化，采用 GJ-1 作为外部锆石年龄标准，进行 U-Pb 同位素分馏校正，每

隔 8 个样品，加测 2 个标样各 1 次。原始数据处理采用中国地质大学刘勇胜教授研发的 ICP -MSData Cal 程序（Liu YS et al., 2010），采用^{208}Pb 校正法对普通 Pb 进行校正（Andersen T, 2002），锆石年龄谐和图绘制和年龄权重平均值计算采用 Isoplot 3.0 程序（Ludwig KR, 2003）。

全岩地球化学测试在中国地质调查局天津地质调查中心完成，均选取裂隙较少的新鲜岩石标本，检测依据为 GB/T 14506–2010，测试流程见尹明等（2011）。常量元素采用硼酸锂熔融消解、X 射线荧光光谱法（XRF）测试，FeO 应用氢氟酸–硫酸溶样、重铬酸钾滴定容量法。微量元素和稀土元素采用四酸消解、等离子质谱综合分析（ICP–MS）。

3 数据样本描述

内蒙古北山哈珠地区晚古生代花岗岩类年代学与地球化学测试数据集为 Excel 表格型数据，包括 2 个 Excel 数据文件，分别为“Geochemistry data_HZ.xls”和“Zircon U–Pb dating data_HZ.xls”。其中，“Geochemistry data_HZ.xls”为全岩地球化学数据文件，包括 27 件样品以及样品编号、岩石类型与岩石地球化学信息（表 3）；“Zircon U–Pb dating data_HZ.xls”为锆石 U-Pb 测年数据文件，描述研究区内样品 U-Pb 年龄信息，包括 9 件锆石测年样品，每个样品为一个单独的工作表，每个工作表（sheet）包含样品编号、采样点、岩石类型、分析点号、Th/U 比值、同位素比值、年龄及误差等数据（表 4）。

4 数据质量控制和评估

花岗岩类样品全岩地球化学和锆石 U–Pb 年代学测试均在中国地质调查局天津地质调查中心实验室完成。测试方法与过程均严格按照国标进行。全岩地球化学测试经国家标样 GBW07103 和 GBW07111 监控，常量元素分析精度优于 1%，微量元素和稀土元素分析精度优于 5%。由于北山地区哈珠一带晚古生代花岗岩均遭受了后期岩浆热事件的影响，因此在进行锆石测年之前，先对打磨、抛光后的锆石靶进行反射光、透射光和阴极发光显微照相，目的是为了选取合适的锆石颗粒，并进行分析点位置的标注，避免分析点处于锆石的裂隙或位于包裹体的边界，从而得出无意义的锆石年龄信息。LA–ICP–MS 锆石 U–Pb 测年的实验过程详见 Yuan HL et al.(2004)，实验中采用 GJ–1 作为外部锆石年龄标准，进行 U–Pb 同位素分馏校正。本次测试获得 GJ–1 的^{206}Pb/^{238}U 年龄为 (600.4±1.1) Ma，与 Jackson SE et al. (2004) 分析获得的^{206}Pb/^{238}U 年龄（600.7±1.1) Ma 在误差范围内一致。采用^{208}Pb 校正法对普通 Pb 进行校正（Andersen T, 2002），利用 NIST612 玻璃标样作为外标，计算锆石样品的 Pb、U、Th 含量。所测 U–Pb 数据点基本落入谐和线上或其附近。本数据集所测得的锆石年龄结果可以在区域上与其他学者的数据结果进行对比（潘志龙，2017；杨富林等，2017；赵志雄等，2018）。

5 数据价值

本文汇集了内蒙古北山哈珠地区晚古生代花岗岩类样品的锆石 U-Pb 测年和全岩地球化学测试数据。锆石年代学数据显示该类岩石的形成时代为石炭纪–二叠纪，岩石全岩常量和微量元素数据表明石炭纪花岗岩类为准铝质–弱过铝质、中钾钙碱性系列岩

表 3 岩石地球化学数据表

数据项	数据类型	示例	数据项	数据类型	示例
岩石类型	字符型	二长花岗岩	Sc	浮点型	6.50
样品编号	字符型	PM02YQ19-2	Nb	浮点型	7.47
SiO_2	浮点型	73.94	Ta	浮点型	0.70
TiO_2	浮点型	0.33	Zr	浮点型	141.00
Al_2O_3	浮点型	13.11	Hf	浮点型	4.32
Fe_2O_3	浮点型	0.67	Ga	浮点型	14.30
FeO	浮点型	1.54	U	浮点型	1.82
MnO	浮点型	0.06	Th	浮点型	10.50
MgO	浮点型	0.73	La	浮点型	19.60
CaO	浮点型	1.32	Ce	浮点型	36.00
Na_2O	浮点型	3.64	Pr	浮点型	4.42
K_2O	浮点型	4.15	Nd	浮点型	15.70
P_2O_5	浮点型	0.08	Sm	浮点型	3.11
LOI	浮点型	0.27	Eu	浮点型	0.45
H_2O^+	浮点型	0.20	Gd	浮点型	3.21
CO_2	浮点型	0.05	Tb	浮点型	0.52
δ	浮点型	1.96	Dy	浮点型	3.19
Mg#	浮点型	0.38	Ho	浮点型	0.66
A/CNK	浮点型	1.02	Er	浮点型	1.96
Cr	浮点型	4.29	Tm	浮点型	0.32
Ni	浮点型	3.17	Yb	浮点型	2.27
Co	浮点型	3.67	Lu	浮点型	0.37
Rb	浮点型	135.00	Y	浮点型	20.00
Cs	浮点型	6.20	REE	浮点型	111.78
Sr	浮点型	134.00	δEu	浮点型	0.43
Ba	浮点型	535.00	$(La/Yb)_N$	浮点型	5.83
V	浮点型	31.20			

注：常量元素单位为%；微量元素单位为10^{-6}。

石；稀土元素配分曲线呈现右倾分布特征；岩石富集大离子亲石元素 Rb、Ba、K 等，亏损 Nb、Ta、Ti 等高场强元素，反映了岩浆形成于与俯冲带有关的陆缘弧环境。而与之相伴生的白山组火山岩具有活动陆缘弧的岩石学和地球化学特征，且由北向南（远离蛇绿岩带方向）具有从钙碱性系列向高钾钙碱性系列演化趋势（任云伟等，2019）。区域上，红石山–百合山蛇绿岩带南侧的少斜沟、风雷山、交叉沟地区广泛分布具有活动陆缘弧性质的晚石炭世钙碱性岩浆岩组合（赵志雄等，2015；贾元琴等，2016），以上事实共同揭示了红石山–百合山洋向南俯冲的极性。

二叠纪花岗岩类则表现为高硅、富碱、准铝、贫镁的特征，为中钾–高钾钙碱性系列岩石；该类岩石同样表现为富集大离子亲石元素，亏损高场强元素，但碱性长石花岗岩内发育文象结构，且花岗闪长岩内发育大规模水晶晶洞，指示其就位于伸展环境。牛文超等（2019）获得了百合山蛇绿岩带中最年轻的块体斜长花岗岩的锆石 U–Pb 年龄为

表 4　锆石 U–Pb 同位素测年数据表

数据项		数据类型	示例
样品编号		字符型	PM02TW32.2
采样点		字符型	内蒙古哈珠地区砾石滩一带
岩石类型		字符型	花岗闪长岩
分析点位		字符型	PM02TW32.2.1
含量/$\times10^{-6}$	Th	浮点型	447
	Pb	浮点型	24
	U	浮点型	500
同位素比值	$^{206}Pb/^{238}U$	浮点型	0.89
	1σ	浮点型	0.0413
	$^{207}Pb/^{235}U$	浮点型	0.0005
	1σ	浮点型	0.2957
	$^{207}Pb/^{206}Pb$	浮点型	0.0056
	1σ	浮点型	0.0519
年龄/Ma	$^{206}Pb/^{238}U$	浮点型	0.0009
	1σ	浮点型	261
	$^{207}Pb/^{235}U$	浮点型	3
	1σ	浮点型	263
	$^{207}Pb/^{206}Pb$	浮点型	5
	1σ	浮点型	280

(297.3±1.5) Ma，限定了百合山洋俯冲拼贴的时代下限。而大红山神螺滩一带双堡塘组（$P_{1\text{-}2}s$）角度不整合覆盖在石炭纪白山组之上，底部发育象征沉积间断的底砾岩，表明区域上弧陆碰撞发生于早二叠世。结合本文中二叠纪花岗岩类的岩石学和地球化学特征，进一步表明北山北带在早二叠世中晚期处于伸展构造体制。

6　结论

内蒙古北山哈珠地区晚古生代花岗岩类年代学与地球化学测试数据集是基于 1∶50 000 哈珠幅等 4 幅区域地质调查工作，在野外路线调查和剖面实测的基础上，借助高精度分析测试手段完成的。该数据集为 Excel 表格型数据，包括“Geochemistry data_HZ.xls”与“Zircon U–Pb dating data_HZ.xls”2 个 Excel 数据文件。其中，“Geochemistry data_HZ.xls”数据文件，包括 27 件样品以及样品编号、岩石类型与全岩地球化学信息；“Zircon U–Pb dating data_HZ.xls”为锆石 U–Pb 测年数据文件，描述研究区内样品 U–Pb 年龄信息，包括 9 件锆石测年样品，每个样品数据为一个单独的工作表，包含样品编号、采样点、岩石类型、分析点号、Th/U、同位素比值、年龄及误差等数据。内蒙古北山哈珠地区晚古生代花岗岩类年代学与地球化学测试数据集可以为研究北山地区红石山—百合山洋的俯冲极性及构造演化提供依据与关键性的基础数据。

参考文献

Andersen T. 2002. Correction of common lead in U-Pb analyses that do not report ^{204}Pb[J]. Chemical

Geology, 192: 59−79.

Jackson Simon E, Pearson Norman J, Griffin William L, Belousova Elena A. 2004. The application of laser ablation-inductively coupled plasma-mass spectrometry to in situ U–Pb zircon geochronology[J]. Chemical Geology, 211: 47–69.

Liu YS, Gao S, Hu ZC, Gao CG, Zong KQ, Wang DB. 2010. Continental and Oceanic Crust Recycling induced Melt-Peridotite Interactions in the Trans-North China Orogen: U-Pb Dating, Hf Isotopes and Trace Elements in Zircons from Mantle Xenoliths[J]. Journal of Petrology, 51(1–2): 537−571.

Ludwig KR. 2003. Isoplot/Ex Version 3.00: A Geochronological Toolkit for Microsoft Excel[J]. Berkeley Geochronology Center Special Publication, 4: 1−70.

Whitney DL, Evans BW. 2010. Abbreviations for names of rock-forming minerals[J]. American Mineralogist, 95: 185−187.

Xiao WJ, Mao QG, Windley BF, Han CM, Qu JF, Zhang JE, Ao SJ, Guo QQ, Cleven NR, Lin SF, Shan YH, Li JL. 2010. Paleozoic multiple accretionary and collisional processes of the Beishan orogenic collage[J]. American Journal of Science, 310(10): 1553−1594.

Yuan HL, Gao S, Liu XM, Li HM, Detlef G, Wu FY. 2004. Accurate U-Pb Age and Trace Element Determinations of Zircon by Laser Ablation-Inductively Coupled Plasma-Mass Spectrometry[J]. Geostandards and Geoanalytical Research, 28(3): 353−370.

耿建珍, 李怀坤, 张健, 周红英, 李惠民. 2011. 锆石 Hf 同位素组成的 LA–MC–ICP–MS 测定 [J]. 地质通报, 30(10): 1508−1513.

龚全胜, 刘明强, 李海林, 梁明宏, 代文军. 2002. 甘肃北山造山带类型及基本特征 [J]. 西北地质, 35(3): 28−34.

龚全胜, 刘明强, 梁明宏, 李海林. 2003. 北山造山带大地构造相及构造演化 [J]. 西北地质, 36(1): 11−17.

何世平, 任秉琛, 姚文光, 付力浦. 2002. 甘肃内蒙古北山地区构造单元划分 [J]. 西北地质, 35(4): 30−40.

何世平, 周会武, 任秉琛, 姚文光, 付力浦. 2005. 甘肃内蒙古北山地区古生代地壳演化 [J]. 西北地质, 38(3): 6−15.

胡新茁, 赵国春, 胡新悦, 廖云峰, 程海峰. 2015. 内蒙古北山地区月牙山蛇绿质构造混杂岩带地质特征、形成时代及大地构造意义 [J]. 地质通报, 34(2–3): 425−436.

黄增保, 金霞. 2006. 甘肃红石山地区白山组火山岩地质特征及构造背景 [J]. 甘肃地质, 15(1): 19−24.

贾元琴, 赵志雄, 许海, 王新亮, 刘强, 王金荣. 2016. 北山风雷山地区白山组流纹岩 LA–ICP–MS 锆石 U–Pb 年龄及构造环境 [J]. 中国地质, 43(1): 91−98.

廖云峰, 胡新茁, 程海峰, 徐旭明. 2016. 内蒙古月牙山蛇绿岩的岩石学、地球化学特征及其地质意义 [J]. 地质通报, 35(8): 1243−1254.

卢进才, 牛亚卓, 魏仙样, 陈高潮, 李玉宏. 2013. 北山红石山地区晚古生代火山岩 LA–ICP–MS 锆石 U–Pb 年龄及其构造意义 [J]. 岩石学报, 29(8): 2685−2694.

聂风军, 江思宏, 白大明. 2002. 北山地区金属矿床成矿规律及找矿方向 [M]. 北京: 地质出版社, 1–408.

聂风军, 江思宏, 白大明, 刘妍, 张义, 赵月明, 安存杰, 王新亮, 苏新旭. 2003. 蒙甘新相邻 (北山) 地区

金铜矿床时空分布特征及成矿作用 [J]. 矿床地质, 22(3): 234−245.

牛文超, 辛后田, 段连峰, 王根厚, 赵泽霖, 张国震, 郑艺龙. 2019. 内蒙古北山地区百合山蛇绿混杂岩带的厘定及其洋盆俯冲极性—基于 1∶5 万清河沟幅地质图的新认识 [J]. 中国地质, 46(5): 977−994.

潘志龙, 王硕, 邱振, 张欢, 张金龙, 田粉英, 李庆喆, 季虹. 2017. 内蒙古北山地区咸水沟一带早石炭世红柳园组火山岩地球化学、锆石 U–Pb 年龄及 Hf 同位素特征 [J]. 地质调查与研究, 40(2): 99−108.

任邦方, 段连峰, 李敏, 牛文超, 任云伟. 2020. 内蒙古北山哈珠地区晚古生代花岗岩类年代学与地球化学测试数据集 [DB/OL]. 地质科学数据出版系统. (2020-06-30). DOI:10.35080/data.A.2020.P5.

任云伟, 任邦方, 牛文超, 孙立新, 李敏, 张阔, 张家辉, 段连峰. 2019. 内蒙古哈珠地区石炭纪白山组火山岩: 北山北部晚古生代活动陆缘岩浆作用的产物 [J]. 地球科学, 44(1): 312−327.

孙立新, 张家辉, 任邦方, 牛文超, 任云伟, 张阔. 2017. 北山造山带白云山蛇绿混杂岩的地球化学特征、时代及地质意义 [J]. 岩石矿物学杂志, 36(2): 131−147.

王国强, 李向民, 徐学义, 余吉远, 武鹏. 2014. 甘肃北山红石山蛇绿岩锆石 U–Pb 年代学研究及构造意义 [J]. 岩石学报, 30(6): 1685−1694.

徐学义, 何世平, 王洪亮, 陈隽璐, 张二朋, 冯益民. 2008. 中国西北部地质概论—秦岭、祁连、天山地区 [M]. 北京: 科学出版社, 1–355.

杨富林, 邹运鑫, 曹霞, 杨亮, 马刚, 高鉴. 2017. 内蒙古北山地区蓬勃山南石英闪长岩 LA–ICPMS 锆石 U–Pb 测年及其意义 [J]. 地质调查与研究, 40(2): 109−118.

杨合群, 李英, 李文明, 杨建国, 赵国斌, 孙南一, 王小红, 谭文娟. 2008. 北山成矿构造背景概论 [J]. 西北地质, 41(1): 22−28.

杨合群, 李英, 赵国斌, 李文渊, 王小红, 姜寒冰, 谭文娟, 孙楠一. 2010. 北山蛇绿岩特征及构造属性 [J]. 西北地质, 43(1): 26−36.

尹明, 李家熙. 2011. 岩石矿物分析 (第二分册)[M]. 第四版次. 北京: 地质出版社, 1–862.

赵志雄, 贾元琴, 许海, 王金荣, 王新亮, 刘强. 2015. 北山交叉沟石英闪长岩锆石 LA-ICP-MS U-Pb 年龄及构造意义 [J]. 地质学报, 89(7): 1210−1218.

赵志雄, 贾元琴, 王金荣, 许海, 熊煜, 王新亮, 刘强, 高伟, 高鉴, 刘孟合. 2018. 内蒙古小黑山地区二长花岗岩和石英闪长岩的锆石 U–Pb 年代学、元素地球化学及其地质意义 [J]. 地球科学, 43(S2): 49−59.

左国朝, 何国琦. 1990. 北山板块构造及成矿规律 [M]. 北京: 北京大学出版社, 1–226.

左国朝, 刘义科, 刘春燕. 2003. 甘新蒙北山地区构造格局及演化 [J]. 甘肃地质学报, 12(1): 1−15.

doi: 10.12029/gc2020Z105

Article Citation: Ren Bangfang, Duan Lianfeng, Li Min, Niu Wenchao, Ren Yunwei. 2020. Geochronological and Geochemical Dataset of Late Paleozoic Granitoids in the Hazhu Area of Beishan, Inner Mongolia[J]. Geology in China, 47(S1):54−66.

Dataset Citation: Ren Bangfang; Duan Lianfeng; Li Min; Niu Wenchao; Ren Yunwei. Geochronological and Geochemical Dataset of Late Paleozoic Granitoids in the Hazhu Area of Beishan, Inner Mongolia(V1). Tianjin Center, China Geological Survey[producer], 2014. National Geological Archives of China[distributor], 2020-06-30. 10.35080/data.A.2020.P5; http://dcc.cgs.gov.cn/en//geologicalData/details/doi/10.35080/data.A.2020.P5.

Received: 08-04-2020
Accepted: 27-04-2020

Fund Project:
China Geological Survey Project (DD20160039, DD 20190382)

Geochronological and Geochemical Dataset of Late Paleozoic Granitoids in the Hazhu Area of Beishan, Inner Mongolia

REN Bangfang, DUAN Lianfeng, LI Min, NIU Wenchao*, REN Yunwei

(*Tianjin Center*, *China Geological Survey*, *Tianjin* 300170, *China*)

Abstract: Under the project of '*1∶5 000 Regional Geological and Mineral Survey of the Hazhu*, *Hazhudongshan*, *Hazhunanshan and Lishitan Map-sheet*' by China Geological Survey, this dataset was compiled though rock analysis and tests based on detailed geological field surveys. This paper presents the test data of Late Paleozoic granite samples in the Hazhu area in Beishan, Inner Mongolia. The rock types include tonalite, granodiorite, monzonitic granite and alkaline feldspar granite. Zircon chronological data show that the formative era of these kind of rocks are Carboniferous–Permian. The whole-rock macroelement and trace element data show that Carboniferous granitoids are of the metaluminous-weak peraluminous and medium-K calc-alkaline series. The distribution curve of rare earth elements displays right-leaning characteristics. Trace elements are rich in large-ion lithophile elements including Rb, Ba and K; and deficient in high field-strength elements including Nb, Ta and Ti; thus, indicating that magma was formed in a continental marginal arc environment related to the subduction belt. In contrast, Permian granitoids display high-silicon, alkali-rich, metaluminous and magnesium-deficient features, and constitute a medium-high-K calc-alkaline series. They are also rich in large-ion lithophile elements and deficient in high-field strength elements. However, graphic texture is developed within alkaline feldspar granite and crystal caves are developed on a large scale in granodiorite, indicating that the Permian rock mass is situated in an extensional environment. The combination of the two can provide a basis and fundamental data support for studying the subduction polarity and tectonic evolution of the Hongshishan–Baiheshan Ocean in the Beishan area. This dataset is presented in the form of Excel tables, including two. xls files (Geochemistry data_HZ. Xls and Zircon U–Pb dating

About the first author: REN Bangfang, male, born in 1981, senior engineer, mainly engages in research on basic geology and geochemistry; E-mail: bangfangren@foxmail.com.

The corresponding author: NIU Wenchao, male, born in 1986, engineer, mainly engages in researches on the regional geological survey and orogenic belt; E–mail: billynu2003@163.com.

data_HZ. xls), which record the 27 samples' geochemical data and 11 samples' zircon U–Pb dating results of the samples, respectively. The samples of this dataset were all tested at the Tianjin Center laboratory of China Geological Survey, with reliable data quality.

Key words: Beishan; Hazhu; granite; Carboniferous–Permian; whole-rock geochemical data; zircon U-Pb data

Data service system URL: http://dcc.cgs.gov.cn

1 Introduction

The Beishan orogenic belt is located on the southern margin of the middle section of the Central Asian Orogenic Belt (CAOB), at the intersection of the Tarim–North China Plate, Kazakstan Plate and Siberian Plate (Zuo GC et al., 2003; Fig. 1). Since it has experienced a complicated geological evolutionary process of multi-period and multi-stage plate breakup-subduction-collision-convergence, the tectonic unit division and the closing time frame of the Paleo-Asian Ocean in this area have attracted much attention from scholars at home and abroad (Nie FJ et al., 2002; Gong QS et al., 2003; Xu XY et al., 2008; Xiao WJ et al., 2010; Yang HQ et al., 2010; Lu JC et al., 2013). Previous researchers mainly held four views on the tectonic unit division in the Beishan area:

(1) It is bounded by the Mingshui–Shibanjing–Xiaohuangshan suture zone, with the Kazakhstan Plate in the north and Tarim Plate in the south (Zuo GC et al., 1990);

(2) It is bounded by the Hongliuhe–Niuquanzi–Xichangjing ophiolite belt, with the Tarim Plate in the south and Kazakstan Plate in the north (Xu XY et al., 2008; Yang HQ et al., 2008; Hu XZ et al., 2015; Sun LX et al., 2017);

(3) It is bounded by Hongshishan–Heiyingshan and Liuyuan–Daqishan, and may be classified into the Siberian Plate, Kazakhstan Plate and Tarim Plate from north to south (Nie FJ et al., 2003);

(4) It is bounded by the Hongshishan–Baiheshan–Pengboshan ophiolite belt, with the

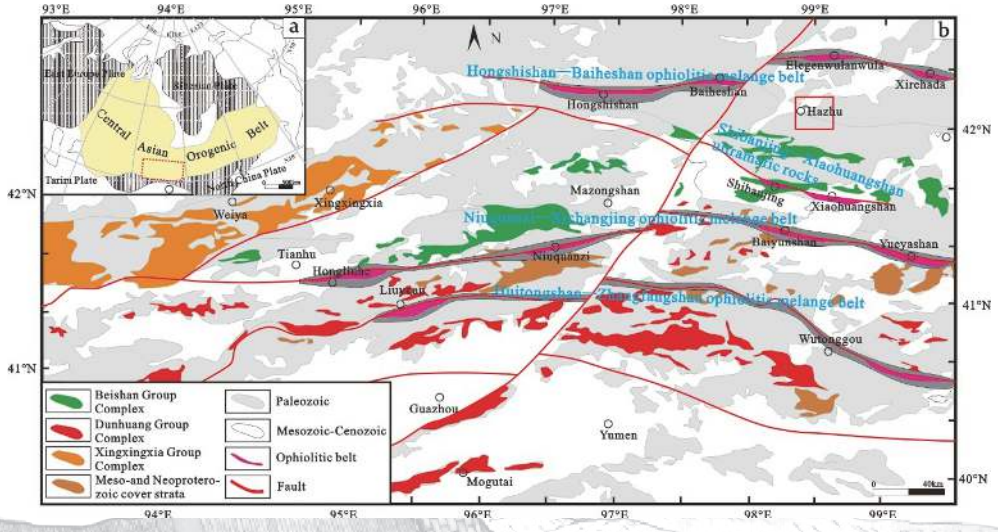

Fig. 1 Tectonic unit division and location of the study area in the Beishan area (Fig. 1a, modified from Xiao WJ et al., 2010; Fig. 1b, modified from Niu WC et al., 2019)

Kazakhstan Plate in the north and Tarim Plate in the south (He SP, 2002; Gong QS et al., 2003).

With the development of geological mapping and investigation in recent years, most scholars have gradually reached a consensus on the tectonic attributes of the Early Palaeozoic ophiolite belt in the Beishan region; with the view that the Hongliuhe–Niuquanzi–Xichangjing ophiolite belt is an Early Palaeozoic suture zone between the Tarim Plate and Kazakstan Plate, with implications for regional tectonic division (Xu XY et al., 2008; Yang HQ et al., 2008; Hu XZ et al., 2015; Liao YF et al., 2016; Sun LX et al., 2017). However, there have always been debates over the tectonic attributes of the Late Paleozoic Hongshishan–Baiheshan ophiolite belt and whether it has the feature of a suture zone (Zuo GC et al., 1990; Gong QS et al., 2002; He SP, 2005; Huang ZB and Jin X, 2006; Yang HQ et al., 2010; Wang GQ et al., 2014).

The studies on magmatic rock exposed on both sides of the Hongshishan-Baiheshan ophiolite belt can effectively facilitate further understanding of the subduction polarity and geological evolution of the Hongshishan–Baiheshan ophiolite belt. This was based on 4 regional geological survey projects, i.e., the 1∶50 000 Hazhu map-sheet, Hazhudongshan map-sheet, Hazhunanshan map-sheet and Lishitan Mmap-sheet. The authors applied high-precision analysis and testing methods in the petrological, geochemical and zircon U–Pb chronological investigations of Late Paleozoic granitoids exposed in the Hazhu area on the south side of the Hongshishan–Baiheshan ophiolite belt, culminating in this dataset.

Late Paleozoic granitoids in the Hazhu area were mainly formed in the Late Carboniferous and Early Permian. The rock types of Late Carboniferous granitoids are mainly tonalite, granodiorite and monzonitic granite, while the rock types of Early Permian granitoids are mainly alkaline feldspar granite, monzonitic granite and granodiorite (Fig. 2). The Late Carboniferous tonalite features a small exposed area and is manifested as stock, intruding into the Lower Carboniferous Lütiaoshan Formation and is intruded by Late Carboniferous granodiorite and Permian granite. The Late Carboniferous granodiorite is developed as a bedrock, distributed in a NW–SE direction and intrudes into the Lutiaoshan Formation and Baishan Formation, within which large quantities of dark basic microparticle inclusions are developed, with mostly distinct boundaries with the host rock, while a few display a transitional relationship. The Late Carboniferous monzonitic granite mainly intrudes into granodiorite, as well as the Lütiaoshan Formation and the Baishan Formation, and is intruded by Early Permian monzonitic granite. Early Permian monzonitic granite and Middle Permian granodiorite are exposed on a large scale and exist in the form of a rock foundation. The two together form a large ellipsoid in open space, of which monzonitic granite is located on both sides of the ellipsoid, granodiorite is located in the center of the ellipsoid and granodiorite intrudes into monzonitic granite (Fig. 3). Subject to regional tectonic influences, the long axis of the ellipsoid is NWW-trending. The intrusives are heavily weathered, with strong features of spherical weathering and cave-shaped wind erosion, forming large numbers of quartz geodes. Dark dioritic inclusions are developed in the intrusives and white coarse-grained feldspar crystals can be seen in some dioritic inclusions. In the study area, Early Permian alkaline

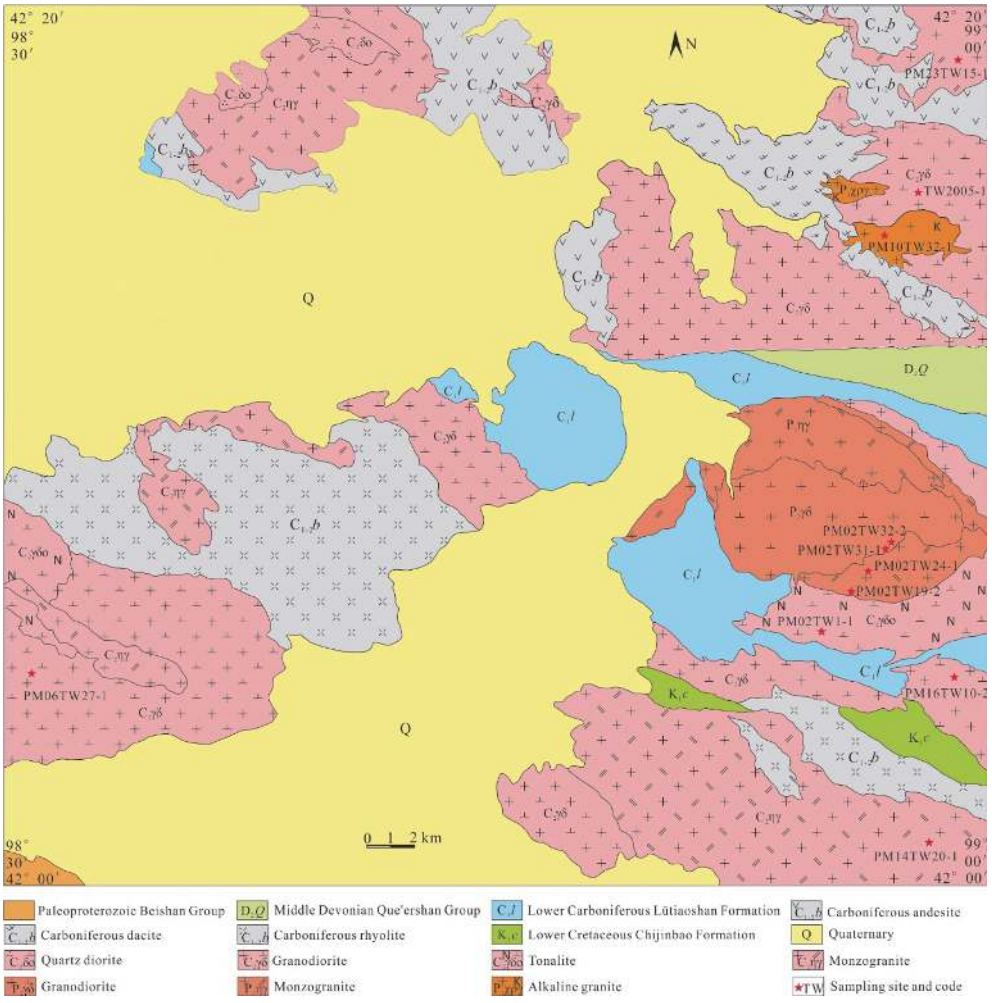

Fig. 2 Geological map of the Hazhu area in Beishan, Inner Mongolia and sampling location for isotopic dating (based on 1∶50 000 regional geological maps including the Hazhu map-sheet, Inner Mongolia)

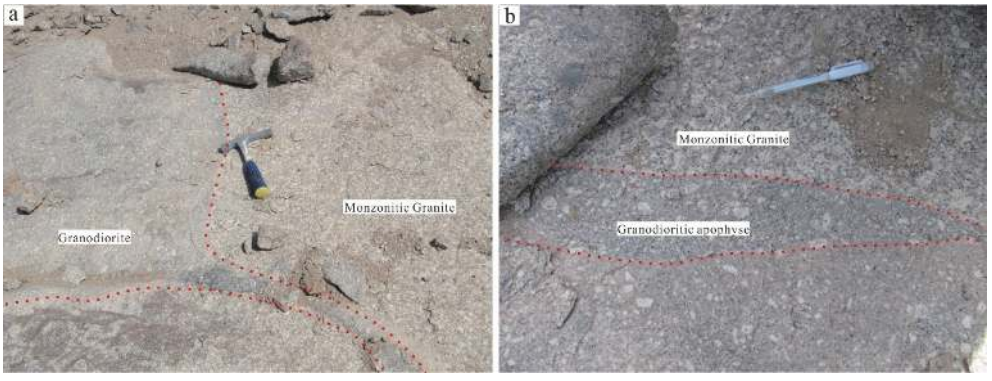

Fig. 3 Contact relation between early Permian granodiorite and monzonitic granite in the Hazhu area in Beishan, Inner Mongolia

a—Granodiorite intruding into monzonitic granite; b—Granodioritic apophyse intruding into monzonitic granite)

feldspar granite has a small exposed area and exists in small stocks, intruding into Carboniferous granite and the volcanic rock of the Baishan Formation.

See Table 1 for the metadata of the zircon chronological and whole-rock geochemical analytical dataset(Ren BF et al., 2020) of Late Paleozoic granitoids in the Hazhu area.

Table 1 Metadata Table of Database (Dataset)

Items	Description
Database (dataset) name	Geochronological and Geochemical Dataset of Late Paleozoic Granitoids in the Hazhu Area of Beishan, Inner Mongolia
Database (dataset) authors	Ren Bangfang, Tianjin Center, China Geological Survey Duan Lianfeng, Tianjin Center, China Geological Survey Li Min, Tianjin Center, China Geological Survey Niu Wenchao, Tianjin Center, China Geological Survey Ren Yunwei, Tianjin Center, China Geological Survey
Data acquisition time	2014—2016
Geographic area	42°00′00″ – 42°20′00″N, 98°30′00″ – 99°00′00″E
Data format	*.xls
Data size	140 kB
Data service system URL	http://dcc.cgs.gov.cn
Fund project	China Geological Survey Project (DD20160039, DD20190382)
Language	Chinese
Database (dataset) composition	The dataset consists of two parts: (1) *geochemical data_HZ.xls* (whole-rock geochemical data) includes 27 samples and their sample codes and rock types; (2) *Zircon U–Pb dating data_HZ.xls* includes 11 samples for zircon U–Pb dating, where each sample represents a separate sheet containing the data of sample code, sampling point, rock type, analysis point number, isotope ratio, age and error

2 Data Acquisition and Processing Methods

2.1 Data Acquisition

The 27 rock samples collected in this study are Late Carboniferous –Early Permian granitoids in the Hazhu area in Beishan, Inner Mongolia. Among these samples, 9 received both zircon U–Pb dating and geochemical analysis, 2 received only zircon U–Pb dating, and 18 received only geochemical analysis. Rock types include tonalite, granodiorite, monzonitic granite and alkaline feldspar granite. The sampling sites and the specific mineral associations are shown in Table 2. The scheme from Whitney DL et al. (2010) was used for the abbreviated name of minerals.

2.2 Sample Collection, Preparation and Testing Methods

Granite samples used for testing in this study were systematically collected on the basis of field route investigation and profile measurement. The preparation of samples and zircon sorting were completed at the laboratory of the Regional Geological and Mineral Resources Survey Institute of Hebei Province, China. The samples were crushed to a 40–60 mesh. After magnetic separation and heavy-liquid separation, zircon particles with clean and good euhedral quality, few inclusions and fissures were manually selected under binocular glasses to make epoxy resin. Target-making and zircon cathodoluminescence photo-taking were conducted at Beijing Gaonianlinghang Technology Co. Ltd. After analysing the appearance of the zircon samples, those with obvious magmatic oscillatory zoning structure and no fissures and inclusions were selected for testing LA-ICP-MS zircon U-Pb isotope determination was carried out at the isotope laboratory of the Tianjin Center of China Geological Survey, using the laser

Table 2 Sampling sites and mineral associations of the granitoids in the Hazhu area

Sample No.	Sampling site	Rock type	Mineral associations
PM02YQ19-2	Lishitan, Hazhu area, Inner Mongolia	Monzonitic granite	kfs(40%±), pl(35%), qtz(20%±), bt(3%±), hbl(2%±)
PM02YQ24-1	Lishitan, Hazhu area, Inner Mongolia	Monzonitic granite	pl(40%±), kfs(30%±), qtz(20%±), bt(5%±), hbl(2%±)
PM02YQ25-2	Lishitan, Hazhu area, Inner Mongolia	Granodiorite	pl(45%±), kfs(25%±), qtz(20%±), hbl(5%±), bt(3%±)
PM02YQ31-1	Lishitan, Hazhu area, Inner Mongolia	Granodiorite	pl(45%±), qtz(35%±), kfs(15%±), hbl(5%±)
PM02YQ32-1	Lishitan, Hazhu area, Inner Mongolia	Granodiorite	pl(50%±), qtz(25%±), kfs(15%±), hbl(5%±), bt(2%±)
PM02YQ32-2	Lishitan, Hazhu area, Inner Mongolia	Granodiorite	pl(50%±), kfs(20%±), qtz(20%±), hbl(5%±), bt(3%±)
PM02YQ33-2	Lishitan, Hazhu area, Inner Mongolia	Granodiorite	pl(45%±), qtz(25%±), kfs(20%±), bt(5%±), hbl(3%±)
PM02YQ38-1	Lishitan, Hazhu area, Inner Mongolia	Granodiorite	pl(50%±), kfs(25%±), qtz(20%±), hbl(5%±), bt(2%±)
PM02YQ39-1	Lishitan, Hazhu area, Inner Mongolia	Monzonitic granite	pl(40%±), kfs(30%±), qtz(20%±), hbl(5%±), bt(3%±)
PM02YQ40-2	Lishitan, Hazhu area, Inner Mongolia	Monzonitic granite	pl(35%±), kfs(35%±), qtz(25%±), hbl(3%±), bt(2%±)
PM02YQ42-1	Lishitan, Hazhu area, Inner Mongolia	Tonalite	pl(55%±), qtz(30%±), bt(8%±), kfs(5%±), hbl(2%±),
PM02YQ44-1	Lishitan, Hazhu area, Inner Mongolia	Tonalite	pl(60%±), qtz(25%±), kfs(5%±), hbl(5%±), bt(5%±)
PM02YQ45-1	Lishitan, Hazhu area, Inner Mongolia	Tonalite	pl(55%±), qtz(30%±), kfs(5%±), hbl(5%±), bt(5%±)
YQ7907-1	Lishitan, Hazhu area, Inner Mongolia	Granodiorite	pl(50%±), qtz(25%±), kfs(20%±), hbl(5%±), bt(2%±)
YQ7965-2	Lishitan, Hazhu area, Inner Mongolia	Granodiorite	pl(45%±), qtz(25%±), kfs(20%±), hbl(5%±), bt(3%±)
PM06YQ20-1	Huzhunanshan, Inner Mongolia	Granodiorite	pl(60%±), qtz(20%±), kfs(15%±), bt(5%±)
PM06YQ27-1	Huzhunanshan, Inner Mongolia	Granodiorite	pl(55%±), qtz(25%±), kfs(15%±), bt(5%±)
PM10YQ32-1	Lishitan, Hazhu Area, Inner Mongolia	Alkaline feldspar granite	af(60%±), qtz(35%±), bt(5%±)
PM16YQ1-1	Huzhunanshan, Inner Mongolia	Granodiorite	pl(40%±), qtz(30%±), hbl(15%±), kfs(10%±), bt(5%±)
PM16YQ2-1	Huzhunanshan, Inner Mongolia	Granodiorite	pl(50%±), qtz(20%±), kfs(10%±), hbl(10%±), bt(8%±)
PM16YQ3-1	Huzhunanshan, Inner Mongolia	Granodiorite	pl(50%±), qtz(20%±), kfs(15%±), hbl(10%±), bt(5%±)
PM16YQ10-1	Huzhunanshan, Inner Mongolia	Granodiorite	pl(55%±), qtz(20%±), kfs(10%±), hbl(10%±), bt(5%±)
PM16YQ10-2	Huzhunanshan, Inner Mongolia	Granodiorite	pl(50%±), qtz(20%±), kfs(10%±), bt(10%±), hbl(8%±)
PM23YQ15-1	Hazhudongshan, Inner Mongolia	Granodiorite	pl(50%±), qtz(20%±), kfs(15%±), hbl(10%±), bt(5%±)
YQ11	Lishitan, Hazhu area, Inner Mongolia	Monzonitic granite	pl(35%±), kfs(35%±), qtz(25%±), hbl(3%±), bt(2%±)
YQ12	Lishitan, Hazhu area, Inner Mongolia	Monzonitic granite	pl(40%±), kfs(30%±), qtz(20%±), hbl(5%±), bt(3%±)
YQ2005-1	Hazhudongshan, Inner Mongolia	Granodiorite	pl(40%±), qtz(30%±), hbl(15%±), kfs(10%±), bt(5%±)

Note: af–alkaline feldspar; bt–biotite; hbl–hornblende; kfs–K-feldspar; pl–plagioclase; qtz–quartz

EWWAVE 193 nm FX, and mass spectrometer NEPTUNE from Thermo Fisher (Geng JZ et al., 2011). The diameter of the laser beam-spot was 35 μm, the frequency was between 8–10 Hz and the laser energy density was 13–14 J/cm^2. Helium was used as the carrier gas of the denuded material. The analysis process is described in Yuan HL et al.(2004). In the experiment, NIST612 glass standard reference materials were used as the external standard for instrument optimization; GJ–1 was used as the external standard for U–Pb isotope fractionation correction. The two standard samples were tested once every 8 samples. The ICP–MSData Cal program, developed by Professor Liu Yongsheng of China University of Geosciences (Liu YS et al., 2010), was used to process the original data and the ^{208}Pb correction method was used to correct ordinary Pb (Andersen T, 2002). The Isoplot 3.0 program was used to draw a Concordia diagram for zircon ages and calculate the weighted average age value (Ludwigb KR, 2003).

The whole-rock geochemical test was completed at the Tianjin Center, China Geological Survey, adopting invariably fresh rock samples with few fissures, in accordance with GB/T 14506–2010. The test process is described in Yin M et al.(2011). Macroelements were melted by lithium borate and tested by X-ray fluorescence spectrometry (XRF); the Hydrofluoric Acid-Sulfuric Acid Method and the Potassium Dichromate Titrimetric Method were adopted for FeO. Tetraacid digestion and inductively coupled plasma mass spectrometry (ICP–MS) were adopted to comprehensively analyse trace elements and rare earth elements.

3 Data Sample Description

The Chronological and Geochemical Dataset of Late Paleozoic Granitoids in the Hazhu Area in Beishan, Inner Mongolia is presented in Excel format, with two Excel files, i.e., 'Geochemistry data_HZ.xls' and 'Zircon U–Pb dating data_HZ.xls', of which the former includes 27 samples and their sample codes, rock types and whole-rock geochemical information (Table 3); and the latter provides descriptions of the U–Pb ages of samples in the study area, including 9 zircon dating samples, each being shown on a separate sheet, including sample code, sampling point, rock type, analysis point number, Th/U ratio, isotope ratio, age and error (Table 4).

4 Data Quality Control and Evaluation

The whole-rock geochemical test and zircon U–Pb dating of granitoid samples were completed at the laboratory of the Tianjin Center of China Geological Survey. The testing method and process were in strict accordance with the national standard. The whole-rock geochemical test was monitored by national standard reference samples GBW07103 and GBW07111, and the analysis accuracy of the macroelements is higher than 1%, while that of trace elements and rare earth elements is higher than 5%.

As the Late Paleozoic granites in the Hazhu area of Beishan were all affected by magmatic thermal events in the later stage, therefore, reflected and transmitted light, and cathodoluminescence microscopy were carried out before zircon dating on polished zircon targets. The purpose is to select suitable zircon particles and mark the location of analysis

Table 3 Data structure of the lithogeochemical data

Data item	Data type	Examples	Data item	Data type	Examples
Rock type	Character	Monzonitic granite	Sc	Float	6.50
Sample code	Character	PM02YQ19-2	Nb	Float	7.47
SiO_2	Float	73.94	Ta	Float	0.70
TiO_2	Float	0.33	Zr	Float	141.00
Al_2O_3	Float	13.11	Hf	Float	4.32
Fe_2O_3	Float	0.67	Ga	Float	14.30
FeO	Float	1.54	U	Float	1.82
MnO	Float	0.06	Th	Float	10.50
MgO	Float	0.73	La	Float	19.60
CaO	Float	1.32	Ce	Float	36.00
Na_2O	Float	3.64	Pr	Float	4.42
K_2O	Float	4.15	Nd	Float	15.70
P_2O_5	Float	0.08	Sm	Float	3.11
LOI	Float	0.27	Eu	Float	0.45
H_2O^+	Float	0.20	Gd	Float	3.21
CO_2	Float	0.05	Tb	Float	0.52
δ	Float	1.96	Dy	Float	3.19
Mg#	Float	0.38	Ho	Float	0.66
A/CNK	Float	1.02	Er	Float	1.96
Cr	Float	4.29	Tm	Float	0.32
Ni	Float	3.17	Yb	Float	2.27
Co	Float	3.67	Lu	Float	0.37
Rb	Float	135.00	Y	Float	20.00
Cs	Float	6.20	REE	Float	111.78
Sr	Float	134.00	δEu	Float	0.43
Ba	Float	535.00	$(La/Yb)_N$	Float	5.83
V	Float	31.20			

Note: The unit of macroelements is %; the unit of trace elements is 10^{-6}.

points in order to prevent them from being located in the cracks of zircon or at the boundary of inclusions and therefore leading to meaningless zircon ages. The experimental process of LA-ICP-MS zircon U–Pb dating is detailed in Yuan HL et al. (2004). In the experiment, GJ–1 was used as the external zircon age standard and U–Pb isotope fractionation correction was implemented. The $^{206}Pb/^{238}U$ age of GJ–1 obtained by this test is 600.4±1.1 Ma, which is consistent with the $^{206}Pb/^{238}U$ age (600.4±1.1 Ma) obtained by Jackson SE et al. (2004). The normal Pb was corrected by the ^{208}Pb correction method (Andersen T, 2002), and the Pb, U and Th contents of zircon samples were calculated by using NIST612 glass reference materials as the external standard. The measured U–Pb data points basically fell on or near the Concordia curve. The zircon age measured in this dataset can be compared with the results of other scholars for the region (Pan ZL, 2017; Yang FL et al., 2017; Zhao ZX et al., 2018).

Table 4 Data structure of the zircon U–Pb isotopic dating data

Data item		Data type	Examples
Sample code		Character	PM02TW32.2
Sampling point		Character	Lishitan, Hazhu Area, Inner Mongolia
Rock type		Character	Granodiorite
Analysis point		Character	PM02TW32.2.1
Content/$\times10^{-6}$	Th	Float	447
	Pb	Float	24
	U	Float	500
Isotope ratio	$^{206}Pb/^{238}U$	Float	0.89
	1σ	Float	0.041 3
	$^{207}Pb/^{235}U$	Float	0.000 5
	1σ	Float	0.295 7
	$^{207}Pb/^{206}Pb$	Float	0.005 6
	1σ	Float	0.051 9
Age/Ma	$^{206}Pb/^{238}U$	Float	0.000 9
	1σ	Float	261
	$^{207}Pb/^{235}U$	Float	3
	1σ	Float	263
	$^{207}Pb/^{206}Pb$	Float	5
	1σ	Float	280

5 Data Value

This paper presents the data of zircon U–Pb dating and whole-rock geochemical test of Late Paleozoic granitoid samples in the Hazhu area in Beishan, Inner Mongolia. Zircon chronological data show that the formative era of these kind of rocks are Carboniferous-Permian. The whole-rock macroelement and trace element data show that Carboniferous granitoids are of the metaluminous–weak peraluminous and medium-K calc-alkaline series. The distribution curve of rare earth elements displays right-leaning characteristics. Trace elements are rich in large-ion lithophile elements including Rb, Ba and K; and deficient in high field-strength elements including Nb, Ta and Ti; indicating that magma was formed in a continental marginal arc environment related to the subduction belt. The associated volcanic rock in the Baishan Formation displays petrological and geochemical characteristics of active continental marginal arc, and a tendency to transition from the calc-alkaline series to high-K calc-alkaline series from north to south (away from the ophiolite zone) (Ren YW et al., 2019). Regionally, the Late Carboniferous calc-alkaline ophiolite assemblage of an active continental marginal arc nature is widely distributed in the Shaoxiegou, Fengleishan and Qiaogou areas on the south side of the Hongshishan-Baiheshan ophiolite zone (Zhao ZX et al., 2015; Jia YQ et al., 2016). The above facts together reveal a southward subduction polarity of the Hongshishan-Baiheshan Ocean.

Permian granitoids display high-silicon, alkali-rich, metaluminous and magnesium-

deficient features, and constitute a medium-high-K calc-alkaline series. They are also rich in large-ion lithophile elements and deficient in high-field strength elements; however, a graphic texture is developed within alkaline feldspar granite, and crystal caves are developed on a large scale in granodiorite, indicating that the Permian rock mass is situated in an extensional environment. Niu WC et al. (2019) obtained a zircon U–Pb age of 297.3±1.5 Ma for the youngest plagiogranite block in the Baiheshan ophiolite zone, thus constraining the lower age limit of the subduction and amalgamation of the Baiheshan Ocean. The angular unconformity of the Shuangbaotang Formation ($P_{1\text{-}2}s$) in the Shenluotan area of Dahongshan overlays the Carboniferous Baishan Formation; while a basal conglomerate, which suggests sedimentary discontinuity, is developed at the bottom, indicating that regional arc-continent collision occurred in the Early Permian. Based on the petrological and geochemical characteristics of the Permian granitoids, this paper further shows that the northern belt of Beishan was situated in an extensional tectonic regime in the middle-late stage of the Early Permian.

6 Conclusion

The Chronological and Geochemical Dataset of Late Paleozoic Granitoids in the Hazhu area in Beishan, Inner Mongolia is based on 1∶50 000 regional geological survey projects including the Hazhu Map-sheet. On the basis of field route investigation and profile measurement, the dataset was completed by means of high-precision analysis and testing. The dataset is presented in Excel format, with two Excel files, i.e. 'Geochemistry data_HZ. xls' and 'Zircon U–Pb dating data_HZ. xls', of which the former includes 27 samples and their sample codes, rock types and whole-rock geochemical information; and the latter provides descriptions of the U–Pb ages of samples in the study area, including 9 zircon dating samples; each being shown on a separate worksheet, including sample code, sampling point, rock type, analysis point number, Th/U, isotope ratio, age and error. The Chronological and Geochemical Dataset of Late Paleozoic Granitoids in the Hazhu area in Beishan, Inner Mongolia can provide a basis and essential basic data for studying the subduction polarity and tectonic evolution of the Hongshishan-Baiheshan Ocean in the Beishan area.

References

Andersen T. 2002. Correction of common lead in U-Pb analyses that do not report 204Pb[J]. Chemical Geology, 192: 59−79.

Geng Jianzhen, Li Huaikun, Zhang Jian, Zhou Hongying, Li Huimin. 2011. Zircon Hf isotope analysis by means of LA-MC-ICP-MS[J]. Geological Bulletin of China, 30(10): 1508−1513 (in Chinese with English abstract).

Gong Quansheng, Liu Mingqiang, Li Hailin, Liang Minghong, Dai Wenjun. 2002. The type and basic characteristics of Beishan orogenic belt, Gansu[J]. Northwestern Geology, 35(3): 28−34 (in Chinese with English abstract).

Gong Quansheng, Liu Mingqiang, Liang Minghong, Li Hailin. 2003. The tectonic facies and tectonic evolution of Beishan Orogenic Belt, Gansu[J]. Northwestern Geology, 36(1): 11−17 (in Chinese with

English abstract).

He Shiping, Ren Bingshen, Yao Wenguang, Fu Lipu. 2002. The division of tectonic units of Beishan area, Gansu-Inner Mongolia[J]. Northwestern Geology, 35(4): 30−40 (in Chinese with English abstract).

He Shiping, Zhou Huiwu, Ren Bingshen, Yao Wenguang, Fu Lipu. 2005. Crustal Evolution of Palaeozoic in Beishan Area, Gansu and Inner Mongona, China[J]. Northwestern Geology, 38(3): 6−15 (in Chinese with English abstract).

Hu Xinzhuo, Zhao Guochun, Hu Xinyue, Liao Yunfeng, Cheng Haifeng. 2015. Geological characteristics, formation epoch and geotectonic significance of the Yueyashan ophiolitic tectonic Mélange in Beishan area, Inner Mongolia[J]. Geological Bulletin of China, 34(2-3): 425−436 (in Chinese with English abstract).

Huang Zenbao, Jin Xia. 2006. Geological characteristics and its setting for volcanic rocks of Baishan formation in hongshishan area of Gansu province[J]. Gansu Geology, 15(1): 19−24 (in Chinese with English abstract).

Jackson Simon E, Pearson Norman J, Griffin William L, Belousova Elena A. 2004. The application of laser ablation-inductively coupled plasma-mass spectrometry to in situ U–Pb zircon geochronology[J]. Chemical Geology, 211: 47−69.

Jia Yuanqin, Zhao Zhixiong, Xu Hai, Wang Xinliang, Liu Qiang, Wang Jinrong. 2016. Zircon LA-ICP-MS U-Pb dating of and tectonic setting of rhyolites from Baishan formation in Fengleishan area of the Beishan orogenic belt[J]. Geology in China, 43(1): 91−98 (in Chinese with English abstract).

Liao Yunfeng, Hu Xinzhuo, Cheng Haifeng, Xu Xuming. 2016. Petrological and petrochemical characteristics and geological significance of Yueyashan ophiolite[J]. Geological Bulletin of China, 35(8): 1243−1254 (in Chinese with English abstract).

Liu Yongsheng, GaoShan, Hu Zhaochu, Gao Changgui, Zong Keqing, Wang Dongbing. 2010. Continental and Oceanic Crust Recycling induced Melt-Peridotite Interactions in the Trans-North China Orogen: U-Pb Dating, Hf Isotopes and Trace Elements in Zircons from Mantle Xenoliths[J]. Journal of Petrology, 51(1-2): 537−571.

Lu Jincai, Niu Yazhuo, Wei Xianyang, Chen Gaochao, Li Yuhong. 2013. LA-ICP-MS zircon U-Pb dating of the Late Paleozoic volcanic rocks from the Hongshishan area of the Beishan orogenic belt and its tectonic significances[J]. Acta Petrologica Sinica, 29(8): 2685−2694 (in Chinese with English abstract).

Ludwing KR. 2003. Isoplot/Ex Version 3.00: A Geochronological Toolkit for Microsoft Excel[J]. Berkeley Geochronology Center Special Publication, 4: 1−70.

Nie Fengjun, Jiang Sihong, Bai Daming. 2002. Metallogenic studies and ore prospecting in the conjunctin area of Inner Mongolia autonomous region, Gansu province and Xinjiang Uygur autonomous region(Beishan Mt.), Northwest China[M]. Beijing: Geological Publishing House, 1–408(in Chinese with English abstract).

Nie Fengjun, Jiang Sihong, Bai Daming, Liu Yan, Zhang Yi, Zhao Yueming, An Chunjie, Wang Xinliang, Su Xinxu. 2003. Temporal-Spatial distribution and metallogenic processes of gold and

copper deposits in Inner Mongolia-Gansu-Xinjiang border(Beishan) region[J]. Mineral Deposits, 22(3): 234−245 (in Chinese with English abstract).

Niu Wenchao, Xin Houtian, Duan Lianfeng, Wang Genhou, Zhao Zelin, Zhang Guozhen, Zheng Yilong. 2019. The identification and subduction polarity of the Baiheshan ophiolite mélanges belt in the Beishan area, Inner Mongolia—New understanding based on the geological map of Qinghegou Sheet (1∶50 000)[J]. Geology in China, 46(5): 977−994 (in Chinese with English abstract).

Pan Zhilong, Wang Shuo, Qiu Zhen, Zhang Huan, Zhang Jinlong, Tian Fenying, Li Qingzhe, Ji Hong. 2017. Geochemistry, zircon U-Pb ages and Hf isotopes of the Early Carboniferous Hongliuyuan volcanic rocks in Xianshuigou, Beishan area, Inner Mongolia[J]. Geological Survey and Research, 40(2): 99−108 (in Chinese with English abstract).

Ren Bangfang, Duan Lianfeng, Li Min, Niu Wenchao, Ren Yunwei. 2020. Geochronological and Geochemical Dataset of Late Paleozoic Granitoids in the Hazhu Area of Beishan, Inner Mongolia [DB/OL]. Geoscientific Data & Discovery Publishing System. (2020-06-30). DOI: 10.35080/data.A.2020.P5.

Ren Yunwei, Ren Bangfang, Niu Wenchao, Sun Lixin, Li Min, Zhang Kuo, Zhang Jiahui, Duan Lianfeng. 2019. Carboniferous volcanics from the Baishan formation in the Hazhu area, Inner Mongolia: implications for the late Paleozoic active continental margin magmatism in the northern Beishan[J]. Earth Science, 44(1): 312−327 (in Chinese with English abstract).

Sun Lixin, Zhang Jiahui, Ren Bangfang, Niu Wenchao, Ren Yunwei, Zhang Kuo. 2017. Geochemical characteristics and U-Pb age of Baiyunshan ophiolite mélange in the Beishan orogenic belt and their geological implications[J]. Acta Petrologica et Mineralogica, 36(2): 131−147 (in Chinese with English abstract).

Wang Guoqiang, Li Xiangmin, Xu Xueyi, Yu Jiyuan, Wu Peng. 2014. Ziron U−Pb chronological study of the Hongshishan ophiolite in the Beishan area and their tectonic significance[J]. Acta Petrologica Sinica, 30(6): 1685−1694 (in Chinese with English abstract).

Whitney DL, Evans BW. 2010. Abbreviations for names of rock-forming minerals[J]. American Mineralogist, 95: 185−187.

Xiao WJ, Mao QG, Windley BF, Han C M, Qu J F, Zhang J E, Ao S J, Guo Q Q, Cleven N R, Lin S F, Shan Y H, Li J L. 2010. Paleozoic multiple accretionary and collisional processes of the Beishan orogenic collage[J]. American Journal of Science, 310(10): 1553−1594.

Xu Xueyi, He Shiping, Wang Hongliang, Chen Junlu, Zhang Erpeng, Feng Yiming. 2008. Outline of the Geology of NW China—Qinling, Qilian and Tian Shan Areas[M]. Beijing: Science Press, 1–355(in Chinese).

Yang Fulin, Zou Yunxin, Cao Xia, Yang Liang, Ma Gang, Gao Jian. 2017. Zircon LA-ICPMS U-Pb dating for the quartz diorite in the south Pengboshan of Beishan area, Inner Mongolia[J]. Geological Survey and Research, 40(2): 109−118 (in Chinese with English abstract).

Yang Hequn, Li Ying, Li Wenming, Yang Jianguo, Zhao Guobin, Sun Nanyi, Wang Xiaohong, Tan Wenjuan. 2008. General discussion on metallogenitic tectonic setting of Beishan mountain, Northwestern China[J]. Northwestern Geology, 41(1): 22−28 (in Chinese with English abstract).

Yang Hequn, Li Ying, Zhao Guobin, Li Wenyuan, Wang Xiaohong, Jiang Hanbin, Tan Wenjuan, Sun Nanyi. 2010. Character and structural attribute of the Beishan ophiolite[J]. Northwestern Geology, 43(1): 26−36 (in Chinese with English abstract).

Yin Ming, Li Jiaxi. 2011. Rock and mineral analysis(volume Ⅱ)[M]. Fourth Edition. Beijing: Geological Publishing House, 1–862(in Chinese).

Yuan HL, Gao S, Liu XM, Li HM, Detlef G, Wu FY. 2004. Accurate U-Pb Age and Trace Element Determinations of Zircon by Laser Ablation-Inductively Coupled Plasma-Mass Spectrometry[J]. Geostandards and Geoanalytical Research, 28(3): 353−370.

Zhao Zhixiong, Jia Yuanqin, Xu Hai, Wang Jinrong, Wang Xinliang, Liu Qiang. 2015. LA-ICP-MS zircon U–Pb age of quartz diorite from the Jiaochagou area in Beishan orogenic belt, Inner Mongolia, and its tectonic significance[J]. Acta Geologica Sinica, 89(7): 1210−1218 (in Chinese with English abstract).

Zhao Zhixiong, Jia Yuanqin, Wang Jinrong, Xu Hai, Xiong Yu, Wang Xinliang, Liu Qiang, Gao Wei, Gao Jian. 2018. LA-ICP-MS zircon U –Pb age of monzonite granite-quartz diorite pluton in Xiaoheishan area of Beishan orogenic belt and its geological significance, Inner Mongolia[J]. Earth Science, 43(S2): 49−59 (in Chinese with English abstract).

Zuo Guochao, He Guoqi. 1990. Plate tectonics and metallogenic regularities in Beishan region[M]. Beijing: Peking University Press, 1–226(in Chinese).

Zuo Guochao, Liu Yike, Liu Chunyan. 2003. Framework and evolution of the tectonic structure in Beishan area across Gansu province, Xinjiang autonomous region and Inner Mongolia autonomous region[J]. Acta Geologica Gansu, 12(1): 1−15 (in Chinese with English abstract).